



Published in final edited form as:

Nat Immunol. 2010 December ; 11(12): 1136–1142. doi:10.1038/ni.1960.

Caspase-1-induced pyroptosis is an innate immune effector mechanism against intracellular bacteria

Edward A. Miao¹, Irina A. Leaf¹, Piper M. Treuting², Dat P. Mao¹, Monica Dors¹, Anasuya Sarkar³, Sarah E. Warren^{1,4}, Mark D. Wewers³, and Alan Aderem¹

¹ Institute for Systems Biology, 1441 N 34th St, Seattle, WA 98103, USA

² University of Washington, Department of Comparative Medicine, Seattle, WA 98195, USA

³ The Ohio State University, Davis Heart and Lung Research Institute and Department of Pediatrics, Columbus, OH 43210, USA

⁴ University of Washington, Department of Immunology, Seattle, WA 98195, USA

Summary

Macrophages mediate crucial innate immune responses via caspase-1-dependent processing and secretion of IL-1 β and IL-18. While wild type *Salmonella typhimurium* infection is lethal to mice, a strain that persistently expresses flagellin was cleared by the cytosolic flagellin detection pathway via NLRC4 activation of caspase-1; however, this clearance was independent of IL-1 β and IL-18. Instead, caspase-1 induced pyroptotic cell death, released bacteria from macrophages and exposed them to uptake and killing by reactive oxygen species in neutrophils. Similarly, caspase-1 cleared unmanipulated *Legionella* and *Burkholderia* by cytokine-independent mechanisms. This demonstrates for the first time that caspase-1 clears intracellular bacteria *in vivo* independent of IL-1 β and IL-18, and establishes pyroptosis as an efficient mechanism of bacterial clearance by the innate immune system.

Keywords

Caspase-1; pyroptosis; IL-1 β *Salmonella*; cell death

Macrophages use a compartmentalized dual detection system to respond to bacterial infection. Toll-like receptors (TLRs) respond to extracellular or vacuolar stimuli while Nod-like receptors (NLRs) respond to cytosolic perturbations. In general, the TLRs orchestrate downstream immune responses by inducing the transcription, translation and release of specific cytokines including IL-6 and IL-12. However, in the case of IL-1 β and IL-18 the TLRs and NLRs function in concert. TLRs induce the expression of proIL-1 β and proIL-18,

Users may view, print, copy, download and text and data- mine the content in such documents, for the purposes of academic research, subject always to the full Conditions of use: http://www.nature.com/authors/editorial_policies/license.html#terms

Contact information: Alan Aderem or Edward Miao, Telephone: 206/732-1203 or 206-732-1358, Fax: 206/732-1249 or 206/732-1260, aderem@systemsbiology.org; emiao@systemsbiology.org.

Author Contributions

EAM, IAL, and AA conceived the research plan and wrote the manuscript. EAM, IAL, DPM, MD, AS and MDW planned and performed experiments. PMT planned and performed histological analysis.

following which NLR-dependent activation of caspase-1 regulates their proteolytic processing and release¹.

Many pathogens are controlled by caspase-1-mediated innate immune responses and these are associated with the downstream effects of the pleiotropic cytokines IL-1 β and IL-18². IL-1 β promotes inflammation, including vasodilation and immune cell extravasation, and more recently has been implicated in the generation of T_H17 responses. While IL-18 is best known for its activity in promoting interferon- γ (IFN- γ) production in T_H1 cells, NK cells and cytotoxic T lymphocytes (CTLs), it can also enhance T_H2 cell development and promote local inflammatory responses. Mice deficient in NLRP3 (NLR family, pyrin domain containing 3, also known as cryopyrin) or caspase-1 are more susceptible to influenza infection and this effect is primarily attributable to IL-1 β signaling^{3–7}. In contrast, bacteria such as *Shigella* are controlled by caspase-1-dependent IL-18 secretion, and not IL-1 β secretion⁸. Caspase-1 activation is also involved in autoinflammatory diseases since mutations in NLRP3 that cause spontaneous caspase-1 activation result in a spectrum of cryopyrin-associated periodic fever syndromes. These syndromes can be effectively treated with IL-1 receptor antagonist, indicating that the symptoms are mostly IL-18 independent². Thus, a clear pathway from caspase-1 to IL-1 β or IL-18 is observed in the clearance of several pathogens as well as in autoinflammatory syndromes.

In vitro, in addition to processing IL-1 β and IL-18, caspase-1 activation triggers a form of cell death called pyroptosis⁹. Like apoptosis, pyroptosis requires the proteolytic activation of specific caspases: caspase 3 and 7 for apoptosis and caspase-1 for pyroptosis. In contrast to apoptosis, which is often anti-inflammatory, pyroptosis is predicted to be proinflammatory due to the rapid loss of cell membrane integrity and release of cytosolic contents. Although certain mechanistic aspects have been characterized *in vitro*, the functional role for pyroptosis remains unknown.

Pathogenic bacteria can modulate host cell signaling pathways by delivering virulence factors to the cytosol of host cells. To this end, Type III secretion systems (T3SS) are one of the most complex and versatile mechanisms used by many Gram negative pathogens¹⁰. However, the mammalian innate immune system has developed mechanisms to detect T3SS activity^{1, 11}. SPI1 T3SS, which promotes epithelial cell invasion for *Salmonella typhimurium*, can be readily detected by caspase-1 *in vitro* via NLRC4- (NLR family, CARD domain containing 4; previously called Ipaf) mediated detection of inadvertently translocated flagellin or PrgJ rod protein^{1, 11, 12}. *In vivo*, this detection can delay the kinetics of bacterial replication, but is not sufficient to prevent death of wild type (WT) mice^{13, 14}. *S. typhimurium* express neither SPI1 nor flagellin during the systemic phase of infection. Instead, the bacteria express a different T3SS, SPI2, which promotes replication within macrophages¹⁵. The SPI2 T3SS rod protein, SsaI, is not detected by NLRC4¹². Thus, by repressing both PrgJ and flagellin, *S. typhimurium* is able to evade NLRC4 detection during the systemic phase of infection^{12, 16, 17}.

Here we examine the consequences of NLRC4 and caspase-1 activation on the innate immune response to infection. While WT *S. typhimurium* cause a lethal systemic infection in mice, an *S. typhimurium* strain that fails to evade NLRC4 is efficiently cleared. This

clearance does not require the cytokines IL-1 β and IL-18. Instead, clearance is associated with pyroptotic macrophage cell death. With the lysis of macrophages, pathogens are released into the extracellular space and become exposed to uptake and efficient killing by neutrophils through the activity of reactive oxygen species.

Results

NLRC4 detects flagellin expressing *S. typhimurium*

In vivo, WT *S. typhimurium* (ST-WT) represses flagellin expression and we hypothesized that this increases virulence by enabling evasion of the intracellular flagellin detector, NLRC4. We sought to test this hypothesis by generating an *S. typhimurium* strain that persistently expresses flagellin (*fliC*). This strain, termed 'ST-FliC^{ON}', contains a plasmid in which *fliC* is expressed by a SPI2 promoter. To explore whether ST-FliC^{ON} activates NLRC4, we infected bone marrow derived macrophages (BMDM) with ST-WT or ST-FliC^{ON} and demonstrated that ST-FliC^{ON} induced IL-1 β secretion and caspase-1 processing, whereas ST-WT did not (Fig. 1a, b). These responses required SPI2 T3SS within the bacteria (Fig. 1c) and were dependent on NLRC4 within macrophages (Fig. 1b, 1d).

Flagellin expression attenuates *S. typhimurium in vivo*

To study whether NLRC4 activation impacts systemic bacterial infection *in vivo*, we challenged mice with either ST-WT or ST-FliC^{ON}. WT mice infected with ST-WT succumbed to systemic infection within 6–8 days, whereas ST-FliC^{ON} did not kill WT mice (Fig. 2a). To understand the mechanism underlying the avirulence of ST-FliC^{ON}, we compared bacterial loads of ST-WT and ST-FliC^{ON} in a competitive index (CI) assay. In this assay, equal numbers of a ST-WT reference strain and ST-FliC^{ON} are used to infect the same mouse and bacterial loads of each are determined based on their differential antibiotic resistance (ST-WT in this assay carries kanamycin resistance while ST-FliC^{ON} is resistant to ampicillin). Two days after infection, we recovered 100-fold less ST-FliC^{ON} than ST-WT (yielding the CI value: $\log_{10}\text{Amp/Kan} = -2.00$, Fig. 2b). In contrast, when ampicillin resistant ST-WT were competed against kanamycin resistant ST-WT, there was equal recovery (CI = 0.0, Fig. 2b, for detailed colony forming unit (CFU) data from this and subsequent CI experiments, see Supplementary Table 1). Much fewer ST-FliC^{ON} bacteria were recovered from several target organs, including the draining lymph nodes, the liver and the spleen, with a more pronounced competitive index difference over time (Fig. 2c). As expected, this clearance was dependent upon the SPI2 T3SS (Fig. 2b), consistent with previous observations that T3SS is required for delivery of flagellin to the cytosol¹. Thus, flagellin expression concomitant with SPI2 T3SS expression enables the innate immune system to clear these bacteria.

ST-FliC^{ON} clearance is independent of IL-1 β and IL-18

NLRC4 is required for detection of cytosolic flagellin and subsequent activation of caspase-1 *in vitro*. Similarly, *in vivo*, *Nlr4c*^{-/-} mice succumbed to infection with ST-FliC^{ON} unlike WT mice (Fig. 2a). Consistent with this observation *Nlr4c*^{-/-} and *Casp1*^{-/-} mice failed to clear ST-FliC^{ON} *in vivo* (Fig. 2d, e), while mice deficient for the extracellular flagellin receptor TLR5 had no effect (Fig. 2f). These results also indicate that the *fliC*

expression plasmid does not otherwise interfere with *S. typhimurium* virulence by compromising SPI2 T3SS function or placing a greater metabolic burden on replicating bacteria.

Because caspase-1 is essential for protection, we addressed whether its substrates IL-1 β and/or IL-18 play a role in clearing ST-FliC^{ON}. *Il1r1*^{-/-} mice cleared ST-FliC^{ON} equivalent to that seen in wild type mice (Fig. 2g). IL-18 induces the secretion of IFN- γ , which is crucial for late control of ST-WT; however, both *Il18*^{-/-} and *Ifng*^{-/-} mice successfully cleared ST-FliC^{ON} (Fig. 2g, h). Finally, a redundant effect of IL-1 β and IL-18 was also ruled out because mice deficient for both IL-1 β and IL-18 (*Il1b-Il18*^{DKO}), or IL-1R1 and IL-18 (*Il1r1-Il18*^{DKO}) mice also cleared ST-FliC^{ON} (Fig. 2i, j). *Il1b-Il18*^{DKO} mice cleared ST-FliC^{ON} at 24, 48, and 72 hours post infection at rates equal to that seen in WT mice (Supplementary Fig 1a), and were protected from lethal infection by ST-FliC^{ON}, unlike *Nlr4c*^{-/-} mice (Supplementary Fig 1b, Fig. 2a). Cytokine-dependent effects were also observed. *Il1b-Il18*^{DKO} mice showed a mildly increased susceptibility to both ST-WT and ST-FliC^{ON} at 72h post infection (Supplementary Fig 1c, d). However, this difference was significantly lower than the cytokine-independent effect, which enabled greater clearance of ST-FliC^{ON} in both WT and *Il1b-Il18*^{DKO} mice (Supplementary Fig 1c, d). It has been reported that TIRAP, an adaptor protein for TLR signaling, can be cleaved by caspase-1¹⁸, however, *Tirap*^{-/-} mice also cleared ST-FliC^{ON} (Supplementary Fig 1e). These results indicate that NLRC4 and caspase-1 are required for flagellin-induced bacterial clearance, and that this clearance is independent of IL-1 β and IL-18.

Cytokine independent *Legionella* and *Burkholderia* control

The studies described above utilize modified strains of *S. typhimurium* that expresses flagellin *in vivo* as a tool to probe caspase-1 mediated bacterial clearance. We also wished to determine if caspase-1 clears non-modified bacteria from tissues through mechanisms that do not require IL-1 β and IL-18. We therefore examined infection with two bacteria which activate caspase-1 and which reside within macrophages: *Legionella pneumophila* and *Burkholderia thailandensis*. *L. pneumophila* is the causative agent of Legionnaire's disease, while *B. thailandensis* is a model organism for *B. pseudomallei* and *B. mallei*, which cause melioidosis and glanders, respectively. Both *L. pneumophila* and *B. thailandensis* are flagellated and express T4SS and T3SS, respectively.

Mice were infected with either *L. pneumophila* or *B. thailandensis* and colonization of the draining lymph nodes were assessed 24 hours later. In both cases, *Casp1*^{-/-} mice were deficient in their ability to restrict bacterial counts (Fig. 2k, 2l); this effect was not completely recapitulated in *Il1b-Il18*^{DKO} mice (Fig. 2k, l). In *L. pneumophila* infections, *Il1b-Il18*^{DKO} mice had bacterial counts that were significantly higher than WT mice, but also significantly lower than *Casp1*^{-/-} mice (Fig. 2k), suggesting that both cytokine-dependent and -independent control occurs through caspase-1. In *B. thailandensis* infections, bacterial counts in *Il1b-Il18*^{DKO} mice were not statistically different from WT mice, and both were lower than counts observed in *Casp1*^{-/-} mice (Fig. 2l). These results indicate that caspase-1 controls the dissemination of *L. pneumophila* and *B. thailandensis* at or before the

draining lymph node, and the full effect cannot be attributed to the cytokines IL-1 β and IL-18.

ST-FliC^{ON} clearance is independent of ASC

The adaptor protein ASC (apoptosis-associated speck-like protein containing a CARD, also called PYCARD) contains a pyrin and a CARD domain, and is essential to bridge the pyrin of NLRP3 to the CARD of caspase-1¹. In contrast, NLRC4 contains a CARD that directly interacts with the CARD of caspase-1, but nevertheless, ASC enhances NLRC4 dependent caspase-1 activation and IL-1 β secretion^{17, 19–22}. *Asc*^{-/-} mice cleared ST-FliC^{ON} as efficiently as WT mice (Fig. 3a, and Supplementary Fig 1b. This indicates that *in vivo*, ASC signaling is dispensable for NLRC4 and caspase-1-dependent clearance of intracellular pathogens. Interestingly, while ASC enhanced NLRC4-dependent secretion of IL-1 β by bone marrow-derived macrophage (BMDM) after infection with ST-FliC^{ON} *in vitro* (Fig. 3b), it did not contribute to macrophage cell death (Fig. 3c). This cell death in response to ST-FliC^{ON}, was not observed in BMDM infected with ST-WT (Fig. 3d), and showed signs consistent with pyroptosis: it was inhibited by glycine, and dependent on NLRC4 (Fig. 3c, 3e). Thus, ASC enhances NLRC4 dependent IL-1 β secretion but does not contribute to NLRC4-induced pyroptosis, consistent with several prior reports on the role of ASC downstream of NLRC4 activation *in vitro*^{19–22}. Because, ASC and IL-1 β are required for neither pyroptosis *in vitro* nor ST-FliC^{ON} clearance *in vivo*, we hypothesized that caspase-1 dependent ST-FliC^{ON} clearance *in vivo* is mediated by pyroptosis.

Clearance via NLRC4 is associated with pyroptosis

In order to investigate the role of pyroptosis in the clearance of flagellin-expressing bacteria *in vivo*, we synchronized the induction of NLRC4 activation by engineering a *S. typhimurium* strain with inducible flagellin expression (ST-FliC^{IND}). ST-FliC^{IND} contains a plasmid which encodes *fliC* under the control of a doxycycline inducible promoter. Mice were infected with doxycycline resistant, GFP-expressing, ST-WT or ST-FliC^{IND} for 48 hours. Flagellin expression was synchronously induced by intraperitoneal injection of doxycycline, resulting in the progressive clearance of ST-FliC^{IND} (Fig. 4a). Pyroptosis is characterized by the insertion of pores into the plasma membrane of macrophages, which can be detected by propidium iodide staining. ST-FliC^{IND} induced significantly more pyroptosis than ST-WT *in vivo* dependent on NLRC4 detection (Fig. 4b, c). These results suggest that activation of NLRC4 by flagellin *in vivo* induces pyroptosis and that this is temporally correlated with bacterial clearance.

Phagocyte oxidase acts downstream of NLRC4

ST-WT survive and replicate within macrophages and we hypothesized that activation of NLRC4 dependent pyroptosis would result in the release of ST-FliC^{ON} from macrophages, which would expose them to phagocytosis and killing by neutrophils (Supplementary Fig 2). A major antibacterial mechanism utilized by neutrophils is the generation of reactive oxygen species (ROS) by an NADPH oxidase. Mutation of p47^{phox} (encoded by neutrophil cytosolic factor 1, *Ncf1*) one of the subunits of the oxidase complex, abrogates ROS production resulting in mice that are defective in neutrophil killing²³. In our competitive index assay

more ST-FliC^{ON} were recovered than ST-WT in *Ncf1*^{-/-} mice (Fig. 5a). Therefore, in the absence of NADPH oxidase, ST-FliC^{ON} not only regain their normal virulence, but become hypervirulent when compared to ST-WT. This finding is consistent with our prediction that extracellular ST-FliC^{ON} bacteria that are expelled from dying macrophages are exposed and killed by neutrophils via an ROS-dependent mechanism.

NLRC4 activation releases bacteria from macrophages

The observation that neutrophils kill ST-FliC^{ON} is consistent with our model that NLRC4-dependent pyroptosis results in the release of bacteria from macrophages and their subsequent phagocytosis and degradation by neutrophils (Supplementary Fig. 2). The release step of the model was tested by using the membrane impermeant antibiotic gentamicin to differentiate between intracellular and extracellular bacteria *in vivo* in *Ncf1*^{-/-} mice; gentamicin killing substitutes for neutrophil killing after bacterial release. Consistent with our hypothesis, induction of flagellin expression in ST-FliC^{IND} resulted in exposure to gentamicin (Fig. 5b). As a control, gentamicin did not alter the recovery of ST-WT (Fig. 5c). These results indicate that ST-WT are protected from neutrophils by residing within macrophages whereas ST-FliC^{IND} are released from macrophages via pyroptosis.

ST-FliC^{ON} reside predominantly in neutrophils

We next examined the relative number of ST-WT or ST-FliC^{ON} in splenic macrophages (F4/80 positive) and neutrophils (Ly6G positive) in WT and *Ncf1*^{-/-} mice. As expected, ST-FliC^{ON} bacteria were cleared in WT mice and were therefore not detected in macrophages or neutrophils (Fig. 6a). ST-WT were present in similar numbers in neutrophils and macrophages in both WT and *Ncf1*^{-/-} mice (Fig. 6a). Conversely, ST-FliC^{ON} was predominantly found in neutrophils in *Ncf1*^{-/-} mice (Fig. 6a, b), resulting in an increase in the ratio of infected neutrophils to macrophages (Fig. 6c). This skewing into neutrophils was not observed in NLRC4 or Caspase-1 deficient mice (Fig. 6c). NLRC4 was not expressed in neutrophils (Fig. 6d–f), therefore this flagellin detector is likely to be exerting its effect in macrophages.

We examined the pathology of WT and *Ncf1*^{-/-} mice infected with either ST-WT or ST-FliC^{ON}. WT mice infected with ST-WT showed more severe inflammatory changes in the spleen (Fig. 7a) than did WT mice infected with ST-FliC^{ON} (Fig. 7b). *Ncf1*^{-/-} mice infected with ST-WT also showed severe inflammatory changes in the spleen (Fig. 7c, e). The consequences of sustained NLRC4 activation by ST-FliC^{ON} in *Ncf1*^{-/-} mice were more severe including massive necrosis and disruption of normal splenic architecture in *Ncf1*^{-/-} mice (Fig. 7d, e) that was disproportionate to the bacterial counts (Fig. 7f). Taken together, these results suggest that in wild type mice, pyroptosis is beneficial to the host, but that in the absence of downstream killing by neutrophils, repeated rounds of pyroptosis can cause significant damage to host tissues.

Discussion

The innate immune system possesses potent antimicrobial activities, and successful pathogens must evade these defense mechanisms. For example, *S. typhimurium* avoids

multiple innate immune mechanisms, including lipocalin²⁴, antimicrobial peptides²⁵, antigen presentation²⁶, T cell activation²⁶, and as we now show, pyroptosis. An understanding of the evasion strategies used by pathogens can be used to probe the relative importance of specific immune mechanisms. In this study, we have deprived *S. typhimurium* of its NLRC4 evasion strategy, and this has revealed a number of novel insights into innate immune responses to pathogens *in vivo*.

Our first surprise was the observation that the vast majority of caspase-1-dependent clearance of flagellin expressing *S. typhimurium*, *L. pneumophila* and *B. thailandensis* was independent of IL-1 β and/or IL-18. This finding led us to investigate the cytokine-independent mechanisms by which caspase-1 could promote bacterial clearance. In the case of *S. typhimurium* persistently-expressing flagellin, caspase-1-dependent control of infection occurs via pyroptosis-mediated bacterial release followed by neutrophil-dependent killing. *Casp1*^{-/-} mice are more susceptible to infection with *Francisella tularensis* and the use of depleting antibodies to IL-1 β and IL-18 only partially recapitulates the phenotype²⁷. It will be interesting to investigate the role of pyroptosis in this and other infectious model systems.

Different forms of cell death can be categorized in several ways, including programmed or accidental, caspase-dependent or -independent, and inflammatory or non-inflammatory²⁸. Pyroptotic cell death is programmed, caspase-1-dependent, and pro-inflammatory⁹. Apoptosis is also programmed, but in contrast to pyroptosis, it is caspase 3 and 7 dependent and non-inflammatory. Apoptotic cell death results in the orderly degradation and clearance of cellular contents whereas pyroptosis, like necrosis, releases cellular contents into the extracellular environment. The role of pyroptosis *in vivo* has been unclear. It was initially proposed to be a pathogenic mechanism used by bacteria to destroy host immune cells²⁹. However, our data suggests that pyroptosis can be a host defense mechanism used to clear intracellular pathogens.

Several other inflammasome activators in addition to NLRC4 have been shown to induce pyroptosis *in vitro* and in each case, it is easy to envisage how this might promote pathogen clearance. For example, AIM2 detects cytosolic DNA released by viruses³⁰ and by lysed *L. monocytogenes* or *F. tularensis*³¹⁻³⁸, and resulting pyroptosis could prevent replication in macrophages and dendritic cells. Similarly, NLRP3 responds to intracellular bacterial pathogens, including *Listeria monocytogenes*³⁹, as well as to several viruses; again NLRP3-dependent pyroptosis of their host cells could limit their replication. NLRP3 also responds to pore-forming toxins, including those expressed by *Staphylococcus aureus*^{40, 41}, and, in this case, pyroptosis could remove the intoxicated cell.

The inflammasome is also activated by non-infectious stimuli including monosodium urate, asbestos and silica crystals. In these cases pyroptosis may cause pathology by releasing inflammatory mediators from the cell, and this would be significantly exacerbated by cyclical uptake and release of these indigestible crystals. We observe evidence for pyroptosis-induced tissue damage in *Ncf1*^{-/-} mice infected with ST-FliC^{ON}. Our data suggest that in these mice ST-FliC^{ON} cause repeated cycles of pyroptosis and that this results in disruption of splenic architecture and extensive tissue necrosis. In contrast, WT mice rapidly clear ST-FliC^{ON} through pyroptosis without disruption of normal splenic architecture.

Greater numbers of ST-FliC^{ON} are recovered from *Ncf1*^{-/-} mice than ST-WT. Further, we observed that the ST-FliC^{ON} bacteria move from the macrophage to neutrophil compartments. These data suggest that, in the absence of ROS, ST-FliC^{ON} actually replicate within neutrophils, which lack NLRC4 and do not undergo pyroptosis, opening the possibility that replication within ROS-deficient neutrophils is more efficient than replication in macrophages. Alternately, ST-FliC^{ON} may also be replicating in the extracellular space after pyroptotic release, while ST-WT remain relatively more restricted to the macrophage compartment.

Our data indicate that WT *S. typhimurium* efficiently evade NLRC4 and caspase-1 during systemic infection, resulting in the lethal infection in WT mice. *Casp1*^{-/-} or *Il1b-Il18*^{DKO} mice have modestly increased susceptibility to infection with WT *S. typhimurium* suggesting that this evasion may not be complete during every stage of the infection^{13, 14} (Supplementary Fig. 1c, 1d). This detection of WT *S. typhimurium* does not prevent lethality, rather it delays it; WT mice still succumb to infection with WT *S. typhimurium* despite the presence of functional caspase-1^{13, 14}. Caspase-1 activation *in vivo* by WT *S. typhimurium* occurs via both NLRC4 and NLRP3⁴², and the delayed mortality is mediated predominantly by IL-18 with a smaller contribution from IL-1 β ¹⁴. While the molecular mechanisms of NLRP3 detection remain to be elucidated, detection of WT *S. typhimurium* by NLRC4 may arise from the delivery of residual flagellin and PrgJ rod protein present in bacteria located at or just beyond the epithelial barrier in the intestine during the early hours of the infection. Once the bacteria have replicated within host cells, more complete repression of flagellin and PrgJ expression could result in complete evasion of NLRC4 during the systemic phase of the infection.

Our results suggest that caspase-1 activation by WT *S. typhimurium* is relatively weak or transitory, resulting in IL-1 β and IL-18 secretion and a mild reduction in bacterial load that does not prevent mortality. In contrast, persistent and strong caspase-1 activation by ST-FliC^{ON} during the systemic phase of infection enables a dramatic reduction in bacterial counts, resulting in an inability to cause a lethal infection. ST-FliC^{ON} have a major reduction in their virulence, with competitive index values similar SPI2 T3SS mutant and more severe than PhoP mutant *S. typhimurium*⁴³. Thus, while IL-1 β and IL-18 confer a slight delay in mortality after WT *S. typhimurium* infection, WT *S. typhimurium* evade pyroptosis, an innate immune effector mechanism that would otherwise confer complete protection to the host.

In summary, we report two major findings. First, we demonstrate that caspase-1 can clear intracellular pathogens independent of its two primary cytokine substrates, IL-1 β and IL-18. Second, we show that caspase-1 mediates bacterial clearance via an efficient mechanism initiated by pyroptotic cell death. The relative contributions of IL-1 β , IL-18, and pyroptosis to clearing a specific pathogen will likely be different between pathogens, depending on the virulence strategy used and cell types targeted. Further characterization of the role of pyroptosis *in vivo* may lead to novel therapies for both infectious and inflammatory diseases.

Methods

Bacterial strains and plasmids

S. typhimurium strains were derived from ATCC 14028s. Strains and plasmids used are listed in Supplementary Table 2.

Macrophage culture and infection

BMDM were isolated as described¹⁷. Macrophages were infected at the indicated MOI, centrifuged for 5 minutes at 233×g, incubated one hour, then washed and 15 µg/ml gentamicin added to the media; total infection times are indicated. Under these infection conditions, the bacteria are in stationary phase, and neither SPI1 nor SPI2 T3SS is expressed by the infecting bacteria; after phagocytosis by macrophages, SPI2 T3SS expression is induced in the vacuole, and activity is observed after 4–6 hours total infection time⁴⁴. 50 ng/ml LPS was added to the infections to normalize TLR activation between different MOIs. Cytotoxicity was determined by LDH assay (CytoTox 96, Promega). IL-1β secretion was determined by ELISA (R&D Systems), with correction for cytotoxicity as described¹⁷. Caspase-1 processing was determined by immunoblot for the p10 fragment (Santa Cruz) as described¹⁷.

Mice and mouse infections

Wild-type C57BL/6 (Charles River Laboratories), *Il1β*^{-/-45}, *Il18*^{-/-} (Jackson Labs # 004130), *IL1r1*^{-/-} (Jackson Labs # 003245), *Ifng*^{-/-} (Jackson Labs # 002287), *Tirap*^{-/-46}, *TLR5*^{-/-47}, *Casp1*^{-/-48}, *Asc*^{-/-19}, *Nlrc4*^{-/-19}, and *Ncf1*^{-/-} (Jackson Labs # 004742) mice on the C57BL6 background were housed in a specific pathogen free facility. All protocols were approved by the Institutional Animal Care and Use Committee at the Institute for Systems Biology and met U.S. National Institutes of Health guidelines for the humane care of animals. For bacterial infections, mice were infected intraperitoneally (IP) with 1×10⁵ *S. typhimurium* with an exception for *Ncf1*^{-/-} mice that were infected at 1×10³ or 1×10⁴, with 2×10⁶ *L. pneumophila*, or 5×10⁶ *B. thailandensis*. For competitive index assays⁴⁹, the inoculum was equally divided between control (kanamycin resistant) and experimental (ampicillin resistant) strains to comprise the above dose. Spleen or mediastinal lymph nodes were homogenized and CFU determined by dilutional plating. Competitive index are presented representing log(experimental CFU/control CFU). Infected tissues were collected at 24, 48 or 72 hours post-infection, homogenized and grown with appropriate antibiotics to enumerate colony forming units. Induction of the tetracycline promoter was accomplished *in vivo* by IP injection of 0.8 mg per mouse doxycycline. Gentamicin was injected IP at 1 mg per mouse.

Cell isolation and flow cytometry

Peritoneal fluid was collected in ice-cold FACS buffer (2mM EDTA, 1% FCS, 5mM glycine in PBS). For flow cytometric analysis of splenocytes, part of the spleen was used to prepare a single cell suspension by incubating with 0.14 Wunsch units of Liberase III enzyme (Roche) for 30 minutes at 37°C. Peritoneal and splenic cells were identified as macrophage (F480-PE, clone Cl:A3-1, Serotec) or neutrophils (Ly6G-PE, clone 1A8, Invitrogen).

Pyroptotic cells were stained with propidium iodide. GFP expressing *S. typhimurium* were used to mark infected cells.

Histology and immunohistochemistry

Spleens were fixed in formalin and embedded in paraffin to generate 5 micron thick sections. Paraffin sections were counterstained with haematoxylin and eosin. Pathology was scored for both the red pulp and white pulp on a 0–4 scale each for necrosis, neutrophil influx, thrombosis, bacteria, and the percent of tissue involved in any manner and in the worst manner, the sum of these scores is presented. The pathology scoring system is outlined in Supplementary Table 3.

Statistical analysis

Statistical analysis was performed using a two tailed t test with unequal variance; p values less than 0.05 were considered significant. Standard deviations are presented except in Supplementary Fig. 1d, where standard error propagation (SquareRoot of (SEM¹² + SEM²²)) and standard error of the mean are displayed.

Supplementary Material

Refer to Web version on PubMed Central for supplementary material.

Acknowledgments

The authors thank David Rodriguez for managing the mouse colony, and members of the Aderem lab for critical review of this manuscript. This work was supported by NIH grants U54 AI057141, and AI052286.

References

1. Miao EA, Andersen-Nissen E, Warren SE, Aderem A. TLR5 and Ipaf: dual sensors of bacterial flagellin in the innate immune system. *Semin Immunopathol.* 2007; 29:275–288. [PubMed: 17690885]
2. Dinarello CA. Immunological and inflammatory functions of the interleukin-1 family. *Annu Rev Immunol.* 2009; 27:519–550. [PubMed: 19302047]
3. Szretter KJ, et al. Role of host cytokine responses in the pathogenesis of avian H5N1 influenza viruses in mice. *J Virol.* 2007; 81:2736–2744. [PubMed: 17182684]
4. Schmitz N, Kurrer M, Bachmann MF, Kopf M. Interleukin-1 is responsible for acute lung immunopathology but increases survival of respiratory influenza virus infection. *J Virol.* 2005; 79:6441–6448. [PubMed: 15858027]
5. Kozak W, et al. Thermal and behavioral effects of lipopolysaccharide and influenza in interleukin-1 beta-deficient mice. *Am J Physiol.* 1995; 269:R969–977. [PubMed: 7503324]
6. Van Der Sluijs KF, et al. Enhanced viral clearance in interleukin-18 gene-deficient mice after pulmonary infection with influenza A virus. *Immunology.* 2005; 114:112–120. [PubMed: 15606801]
7. Liu B, et al. Interleukin-18 improves the early defence system against influenza virus infection by augmenting natural killer cell-mediated cytotoxicity. *J Gen Virol.* 2004; 85:423–428. [PubMed: 14769900]
8. Sansonetti PJ, et al. Caspase-1 activation of IL-1beta and IL-18 are essential for Shigella flexneri-induced inflammation. *Immunity.* 2000; 12:581–590. [PubMed: 10843390]
9. Bergsbaken T, Fink SL, Cookson BT. Pyroptosis: host cell death and inflammation. *Nat Rev Microbiol.* 2009; 7:99–109. [PubMed: 19148178]

10. Hueck CJ. Type III protein secretion systems in bacterial pathogens of animals and plants. *Microbiol Mol Biol Rev.* 1998; 62:379–433. [PubMed: 9618447]
11. Miao EA, Warren SE. Innate immune detection of bacterial virulence factors via the NLRC4 inflammasome. *J Clin Immunol.* 2010; 30:502–506. [PubMed: 20349122]
12. Miao EA, et al. Innate immune detection of the type III secretion apparatus through the NLRC4 inflammasome. *Proc Natl Acad Sci U S A.* 2010; 107:3076–3080. [PubMed: 20133635]
13. Lara-Tejero M, et al. Role of the caspase-1 inflammasome in *Salmonella typhimurium* pathogenesis. *J Exp Med.* 2006; 203:1407–1412. [PubMed: 16717117]
14. Raupach B, Peuschel SK, Monack DM, Zychlinsky A. Caspase-1-mediated activation of interleukin-1beta (IL-1beta) and IL-18 contributes to innate immune defenses against *Salmonella enterica* serovar Typhimurium infection. *Infect Immun.* 2006; 74:4922–4926. [PubMed: 16861683]
15. Ibarra JA, Steele-Mortimer O. *Salmonella*—the ultimate insider. *Salmonella* virulence factors that modulate intracellular survival. *Cell Microbiol.* 2009; 11:1579–1586. [PubMed: 19775254]
16. Cummings LA, Wilkerson WD, Bergsbaken T, Cookson BT. In vivo, *flhC* expression by *Salmonella enterica* serovar Typhimurium is heterogeneous, regulated by ClpX, and anatomically restricted. *Mol Microbiol.* 2006; 61:795–809. [PubMed: 16803592]
17. Miao EA, et al. Cytoplasmic flagellin activates caspase-1 and secretion of interleukin 1beta via Ipaf. *Nat Immunol.* 2006; 7:569–575. [PubMed: 16648853]
18. Migglin SM, et al. NF-kappaB activation by the Toll-IL-1 receptor domain protein MyD88 adapter-like is regulated by caspase-1. *Proc Natl Acad Sci U S A.* 2007; 104:3372–3377. [PubMed: 17360653]
19. Mariathasan S, et al. Differential activation of the inflammasome by caspase-1 adaptors ASC and Ipaf. *Nature.* 2004; 430:213–218. [PubMed: 15190255]
20. Suzuki T, et al. Differential regulation of caspase-1 activation, pyroptosis, and autophagy via Ipaf and ASC in *Shigella*-infected macrophages. *PLoS Pathog.* 2007; 3:e111. [PubMed: 17696608]
21. Franchi L, et al. Critical role for Ipaf in *Pseudomonas aeruginosa*-induced caspase-1 activation. *Eur J Immunol.* 2007; 37:3030–3039. [PubMed: 17935074]
22. Case CL, Shin S, Roy CR. Asc and Ipaf Inflammasomes direct distinct pathways for caspase-1 activation in response to *Legionella pneumophila*. *Infect Immun.* 2009; 77:1981–1991. [PubMed: 19237518]
23. Sumimoto H, Miyano K, Takeya R. Molecular composition and regulation of the Nox family NAD(P)H oxidases. *Biochem Biophys Res Commun.* 2005; 338:677–686. [PubMed: 16157295]
24. Fischbach MA, et al. The pathogen-associated *iroA* gene cluster mediates bacterial evasion of lipocalin 2. *Proc Natl Acad Sci U S A.* 2006; 103:16502–16507. [PubMed: 17060628]
25. Gunn JS. The *Salmonella* PmrAB regulon: lipopolysaccharide modifications, antimicrobial peptide resistance and more. *Trends Microbiol.* 2008; 16:284–290. [PubMed: 18467098]
26. Bueno SM, Gonzalez PA, Schwebach JR, Kalergis AM. T cell immunity evasion by virulent *Salmonella enterica*. *Immunol Lett.* 2007; 111:14–20. [PubMed: 17583359]
27. Mariathasan S, Weiss DS, Dixit VM, Monack DM. Innate immunity against *Francisella tularensis* is dependent on the ASC/caspase-1 axis. *J Exp Med.* 2005; 202:1043–1049. [PubMed: 16230474]
28. Duprez L, Wirawan E, Vanden Berghe T, Vandenabeele P. Major cell death pathways at a glance. *Microbes Infect.* 2009; 11:1050–1062. [PubMed: 19733681]
29. Zychlinsky A, Prevost MC, Sansonetti PJ. *Shigella flexneri* induces apoptosis in infected macrophages. *Nature.* 1992; 358:167–169. [PubMed: 1614548]
30. Schroder K, Muruve DA, Tschopp J. Innate immunity: cytoplasmic DNA sensing by the AIM2 inflammasome. *Curr Biol.* 2009; 19:R262–265. [PubMed: 19321146]
31. Wu J, Fernandes-Alnemri T, Alnemri ES. Involvement of the AIM2, NLRC4, and NLRP3 inflammasomes in caspase-1 activation by *Listeria monocytogenes*. *J Clin Immunol.* 2010; 30:693–702. [PubMed: 20490635]
32. Warren SE, et al. Cutting edge: Cytosolic bacterial DNA activates the inflammasome via Aim2. *J Immunol.* 2010; 185:818–821. [PubMed: 20562263]

33. Tsuchiya K, et al. Involvement of absent in melanoma 2 in inflammasome activation in macrophages infected with *Listeria monocytogenes*. *J Immunol*. 2010; 185:1186–1195. [PubMed: 20566831]
34. Sauer JD, et al. *Listeria monocytogenes* triggers AIM2-mediated pyroptosis upon infrequent bacteriolysis in the macrophage cytosol. *Cell Host Microbe*. 2010; 7:412–419. [PubMed: 20417169]
35. Rathinam VA, et al. The AIM2 inflammasome is essential for host defense against cytosolic bacteria and DNA viruses. *Nat Immunol*. 2010; 11:395–402. [PubMed: 20351692]
36. Kim S, et al. *Listeria monocytogenes* is sensed by the NLRP3 and AIM2 inflammasome. *Eur J Immunol*. 2010; 40:1545–1551. [PubMed: 20333626]
37. Jones JW, et al. Absent in melanoma 2 is required for innate immune recognition of *Francisella tularensis*. *Proc Natl Acad Sci U S A*. 2010; 107:9771–9776. [PubMed: 20457908]
38. Fernandes-Alnemri T, et al. The AIM2 inflammasome is critical for innate immunity to *Francisella tularensis*. *Nat Immunol*. 2010; 11:385–393. [PubMed: 20351693]
39. Warren SE, Mao DP, Rodriguez AE, Miao EA, Aderem A. Multiple Nod-like receptors activate caspase 1 during *Listeria monocytogenes* infection. *J Immunol*. 2008; 180:7558–7564. [PubMed: 18490757]
40. Craven RR, et al. *Staphylococcus aureus* alpha-hemolysin activates the NLRP3-inflammasome in human and mouse monocytic cells. *PLoS One*. 2009; 4:e7446. [PubMed: 19826485]
41. Munoz-Planillo R, Franchi L, Miller LS, Nunez G. A critical role for hemolysins and bacterial lipoproteins in *Staphylococcus aureus*-induced activation of the Nlrp3 inflammasome. *J Immunol*. 2009; 183:3942–3948. [PubMed: 19717510]
42. Broz P, et al. Redundant roles for inflammasome receptors NLRP3 and NLRC4 in host defense against *Salmonella*. *J Exp Med*. 2010; 207:1745–1755. [PubMed: 20603313]
43. Beuzon CR, Unsworth KE, Holden DW. In vivo genetic analysis indicates that PhoP-PhoQ and the *Salmonella* pathogenicity island 2 type III secretion system contribute independently to *Salmonella enterica* serovar Typhimurium virulence. *Infect Immun*. 2001; 69:7254–7261. [PubMed: 11705895]
44. Miao EA, et al. *Salmonella typhimurium* leucine-rich repeat proteins are targeted to the SPI1 and SPI2 type III secretion systems. *Mol Microbiol*. 1999; 34:850–864. [PubMed: 10564523]
45. Shornick LP, et al. Mice deficient in IL-1beta manifest impaired contact hypersensitivity to trinitrochlorobenzene. *J Exp Med*. 1996; 183:1427–1436. [PubMed: 8666901]
46. Yamamoto M, et al. Essential role for TIRAP in activation of the signalling cascade shared by TLR2 and TLR4. *Nature*. 2002; 420:324–329. [PubMed: 12447441]
47. Uematsu S, et al. Detection of pathogenic intestinal bacteria by Toll-like receptor 5 on intestinal CD11c+ lamina propria cells. *Nat Immunol*. 2006; 7:868–874. [PubMed: 16829963]
48. Kuida K, et al. Altered cytokine export and apoptosis in mice deficient in interleukin-1 beta converting enzyme. *Science*. 1995; 267:2000–2003. [PubMed: 7535475]
49. Beuzon CR, Holden DW. Use of mixed infections with *Salmonella* strains to study virulence genes and their interactions in vivo. *Microbes Infect*. 2001; 3:1345–1352. [PubMed: 11755424]

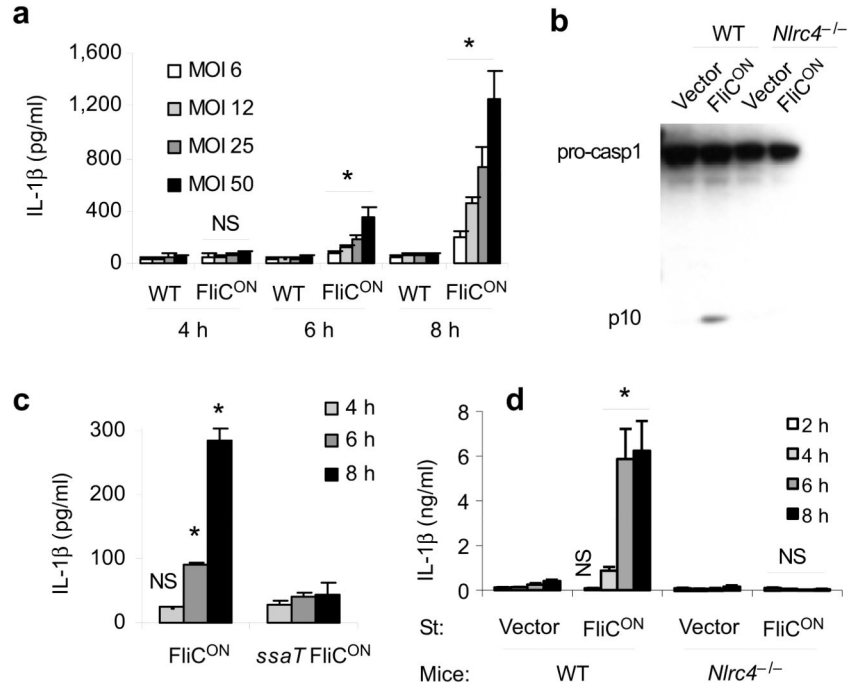


Figure 1. Characterization of flagellin-expressing *S. typhimurium*
(a–d) BMDM were infected with ST-WT or ST-FliC^{ON} under conditions where SPI2 T3SS is expressed and SPI1 T3SS is not expressed at the indicated multiplicity of infection (MOI) for one hour followed by treatment with gentamicin. Total infection time is indicated. **(a)** IL-1β concentration determined by ELISA. **(b)** Caspase-1 processing analyzed by immunoblotting. **(c)** IL-1β concentration after infection with ST-FliC^{ON} or SPI2 mutant ST-FliC^{ON} (*ssa7*) at MOI 12. **(d)** IL-1β concentration after infection of WT or *Nlrc4*^{-/-} BMDM at MOI 10. Data is representative of at least three experiments. * = p < 0.05, NS = p > 0.05 from relevant control.

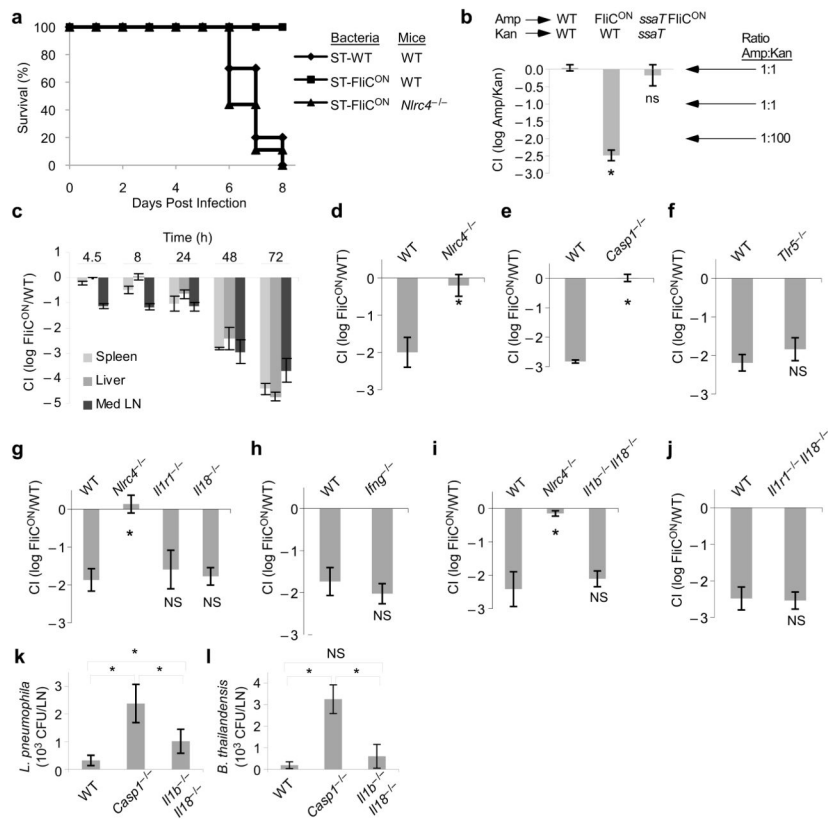


Figure 2. Flagellin expression attenuates *S. typhimurium* in vivo

(a) WT or *Nlrc4*^{-/-} mice were infected with 100 colony forming units (CFU) ST-WT or ST-FliC^{ON} and survival was monitored. (b) WT mice were infected with equal numbers of two bacterial strains marked with different antibiotic markers as indicated. CFU in the spleen were determined after 48h and the log of the ratio is shown as the competitive index. Note that a competitive index of -2 corresponds to a 100-fold reduction in the ampicillin resistant strain. (c) Competitive index of ST-FliC^{ON}/ST-WT in various tissues. (d–j) Competitive index of ST-FliC^{ON}/ST-WT in the indicated WT or knock out mice at 48 h post infection. Samples marked with * are statistically significant from the other samples in the same graph ($p < 0.05$); ns: not significantly different from WT or other samples marked with “ns” ($p > 0.05$). (k, l) WT, *Casp1*^{-/-}, or *Ilr1b*^{-/-}/*Ilr1b*^{-/-} mice were infected intraperitoneally with (k) *L. pneumophila* (data shown from n=4, 6, and 6 mice, respectively, representative of two experiments) or (l) *B. thailandensis* (data shown from n=6, 4, and 6 mice, respectively, representative of four experiments). CFU were enumerated 24 h later from the draining lymph nodes. * = $p < 0.05$, NS = $p > 0.05$. See Supplementary Table 1 for mouse numbers in panels b–j.

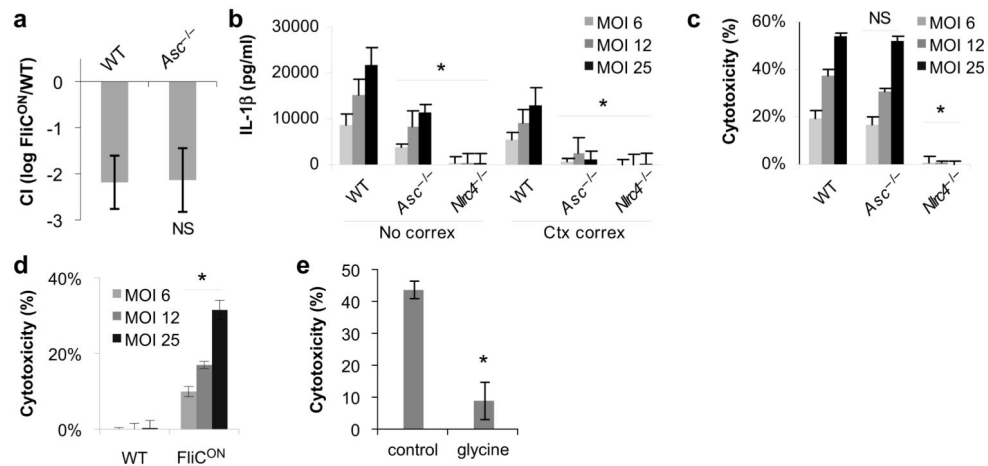


Figure 3. Differential role of ASC in NLRC4 signalling

(a) Competitive index of ST-FliC^{ON} vs. ST-WT as in Figure 2 for WT (n=6) and *Asc*^{-/-} (n=4) mice. (b, c) BMDM from WT, *Asc*^{-/-} or *Nlrp4*^{-/-} mice were infected as in Figure 1 with ST-FliC^{ON} and IL-1 β secretion or cytotoxicity were determined by ELISA and LDH release 6 hours post infection. (d) WT BMDM infected with ST-WT or ST-FliC^{ON} and pyroptosis measured by LDH release 8h post infection. (e) Cytotoxicity induced by ST-FliC^{ON} was monitored with or without 10 mM glycine added to the media and cytotoxicity determined 7h post infection. *In vitro* infections are representative of at least three experiments. * = $p < 0.05$, NS = $p > 0.05$ from relevant control.

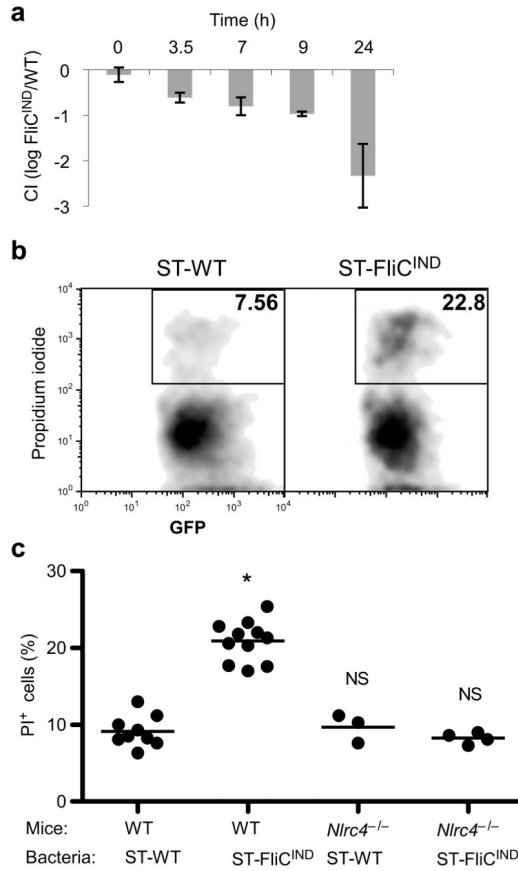


Figure 4. Evidence for pyroptosis *in vivo*

(a–c) Mice were infected with either ST-WT (*flgB* GFP) or flagellin-inducible ST-FliC^{IND} (*flgB* GFP pEM87) for 48 h, after which doxycycline was injected to induce flagellin expression. (a) Competitive index of ST-FliC^{IND}/ST-WT after synchronized induction of flagellin expression (n=2, except 0h n=3). (b–c) GFP-containing cells from the peritoneal wash were analyzed by flow cytometry for membrane integrity by propidium iodide staining (PI). (b) Representative flow cytometry analysis and (c) percent PI positive bacteria containing cells from WT (n=9 and n=11 for ST-WT and ST-FliC^{IND}) or *Nlrc4*^{-/-} (n=3 and n=4 for ST-WT and ST-FliC^{IND}) mice per group, average is shown (bar). * = p < 0.001, NS = p > 0.05.

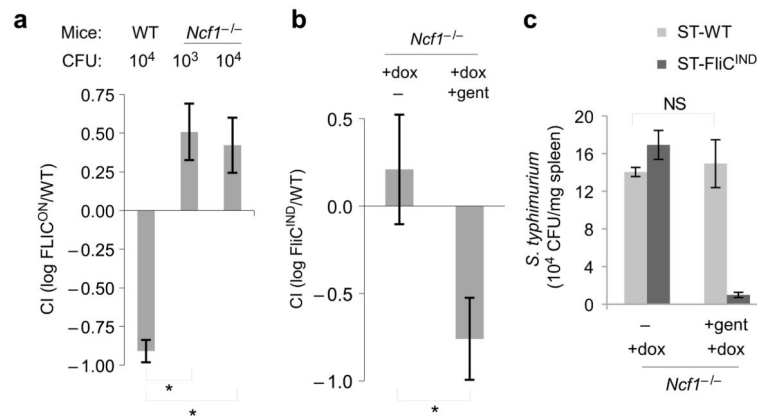


Figure 5. ST-FliC^{ON} are released from macrophages and cleared by ROS

(a) Competitive index of ST-FliC^{ON}/ST-WT 24 h post infection in WT or *Ncf1*^{-/-} mice infected with the indicated inoculum (n=2, except n=3 for *Ncf1*^{-/-} 10³ CFU). (b) Competitive index and (c) individual CFU from coinfection of *Ncf1*^{-/-} mice with ST-FliC^{IND}/ST-WT on a *flgB* mutant background (which ablate endogenous flagellin expression which occurs during growth in LB broth); 24h post infection mice were injected with doxycycline alone (n=8) or doxycycline plus gentamicin (n=10), and CFU were determined 24h later. * = p < 0.05, NS = p > 0.05.

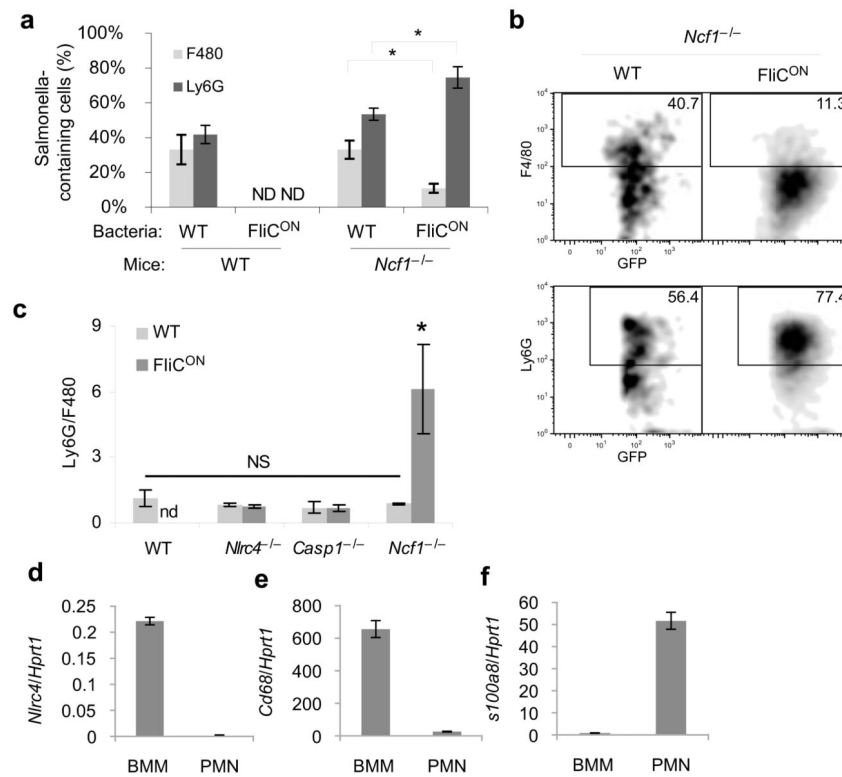


Figure 6. ST-FliC^{ON} accumulate within neutrophils

(a–c) The indicated mouse strains were infected with GFP-expressing ST-WT or ST-FliC^{ON} for 48 hours (n=4 for each; results are representative of three experiments). GFP-containing splenocytes were interrogated for macrophage (F4/80) or neutrophils (Ly6G) markers by flow cytometry. (a) Percent marker positive cells and (b) representative individual plot are shown. (c) Ratio of GFP⁺ Ly6G⁺ to GFP⁺ F4/80⁺ cells determined by flow cytometry. (d–f) qPCR from BMDM or neutrophils (PMNs) for NLRC4, or macrophage (CD68) or neutrophil (S100a8) specific marker controls representative of three experiments. * = p < 0.05, NS = p > 0.05, ND = not detectable.

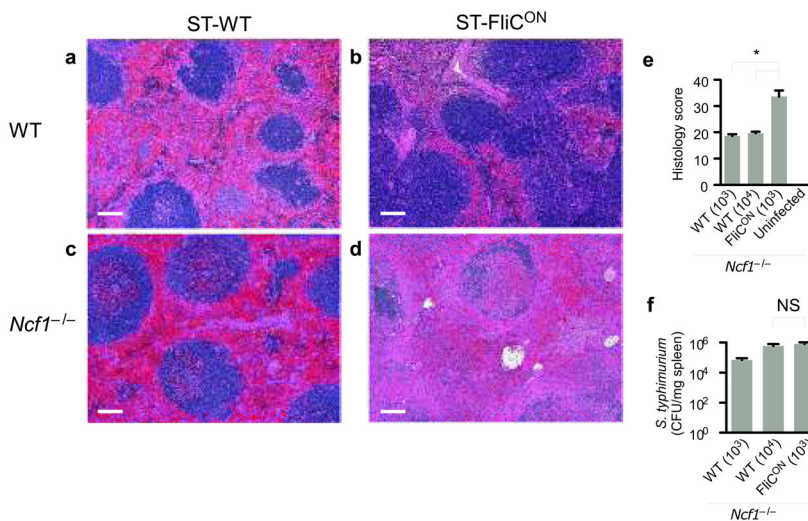


Figure 7. Sustained NLRC4 activation causes tissue damage

WT or *Ncf1*^{-/-} mice were infected with ST-WT or ST-FliC^{ON} for 48 h. WT mice were infected with 10⁵ CFU of each strain. *Ncf1*^{-/-} mice infected with 10³ or 10⁴ CFU ST-WT, or 10³ CFU ST-FliC^{ON}; note that bacterial loads 48h post infection were similar between mice infected with 10⁴ CFU ST-WT and 10³ CFU ST-FliC^{ON} (see f). (a–d) Histopathology of spleens from WT or *Ncf1*^{-/-} mice infected with ST-WT or ST-FliC^{ON}. WT mice infected with ST-WT (a) had multifocal neutrophilic to necrosuppurative splenitis and red pulp congestion. In contrast, WT mice infected with ST-FliC^{ON} (b) had nearly normal splenic morphology. Splenic lesions in the *Ncf1*^{-/-} mice infected with 10³ ST-FliC^{ON} (d) were severe and consisted of marked red and white pulp necrosis. Less severe changes were seen in *Ncf1*^{-/-} mice infected with 10⁴ ST-WT (c), including red pulp congestion, thrombosis, neutrophilic to necrosuppurative splenitis, while the white pulp was relatively spared. Scale bar = 100µm. (e) Scoring of pathologic changes in spleens from *Ncf1*^{-/-} mice (n=3 per inoculum). (f) CFU from the spleen were determined (n=3 per inoculum). Two doses of ST-WT were used in *Ncf1*^{-/-} mice in order to compare to ST-FliC^{ON} infected mice normalized for either initial dose or 48h bacterial load; *Ncf1*^{-/-} infected with 10⁴ CFU ST-WT have similar bacterial loads to *Ncf1*^{-/-} mice infected with 10³ ST-FliC^{ON}. * = p < 0.05, NS = p > 0.05.